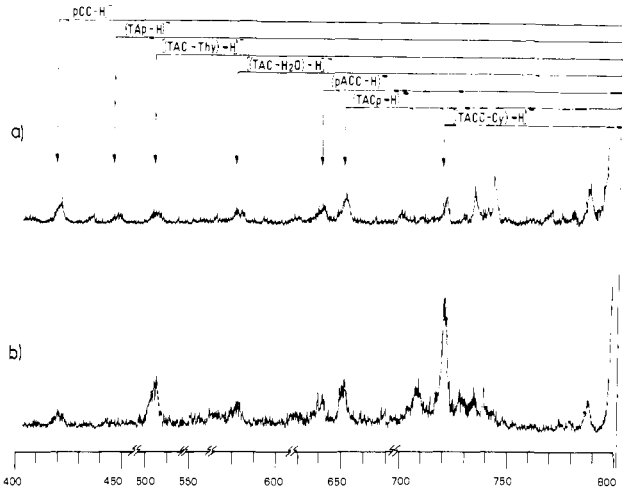

Figure 3. Metastable ion (MI) (a) and collisional activation (CA) (b) secondary mass spectra of d-TACC quasimolecular anion.

and preceding the sputtering process. A very simple view of the structure of those ions might suggest that two phosphodiester acid functions and one monophosphate anion group are present. This, however, is very unlikely since the resulting anion is an amphoteric species bearing two strong acid group ($pK_a = 1$) and hard basic centers such as heterocyclic rings.

Collisional experiments indicate that some of the heterocyclic bases present in the oligomer can be lost as neutrals by a fast single bond cleavage process; therefore, they must contain an extra proton with respect to the original structure of the sampled compound (**1**). Gas-phase data strongly suggest, therefore, a zwitterionic structure for the $(M - H)^-$ obtained after FAB of d-TACC triethylammonium salts; three negative phosphodiester groups and two protonated bases are present, which probably correspond to the cytosine and thymine pyrimidinic rings. The advantage of using a FAB sputtering source to produce gaseous DNA oligomers, rather than other classic MS approaches, relies on the fact that molecules can be released intact in the gas phase with an internal energy content allowing stepwise degradation of the molecule. Thermal procedures, in fact, bring about a complete chemical degradation to sugar, purine and pyrimidine bases before ionization. The application of MS/MS analysis, moreover, allows a specific determination of the breakdown pattern of the ionic species thus produced, in experimental conditions which do not suffer the occurrence of those "hidden variables" often affecting the obtainment of the primary ion spectra by a particle-induced desorption process. Furthermore, the existence of gaseous quasimolecular ions enable the most up-to-date weapons in the mass spectrometrist's armory to be used to fully determine the chemistry involved in a given experiment. This is, in our opinion, a necessary step toward any further applications to the analysis of unknown species.

In conclusion, unprotected deoxyoligonucleotides can be directly sequenced by FABMS from the aqueous solution of their triethylammonium salts, via an investigation of the reactivity of those monoanions possessing a zwitterionic structure. MI determination and CA experiments play a unique role in structure determination and provide a wealth of information which can be used to increase those obtained from the spectra of the primary formed ionic species.

Experimental Section

Oligonucleotides have been synthesized by the phosphotriester approach.[16] The oligomers have been sampled directly from their water solution into the glycerol layer present on the tip of FAB probe. Spectra have been recorded in a double-focusing mass spectrometer VG ZAB equipped with a commercial FAB gun. CA experiments have been performed admitting air in the collision cell of the second field-free region and reducing by a factor of 3 the intensity of the sampled quasimolecular anions.

Acknowledgment. We thank Professor Colin B. Reese for helpful discussions and Miss D. Scott for help with the MS.

Registry No. 1, 86392-57-6; **2**, 86392-58-7.

(16) Reese, C. B. *Tetrahedron* **1978**, *34*, 3143.

Electrochemical and Spectral Characterization of Iron Mono- and Dinitrosyl Porphyrins

D. Lançon and K. M. Kadish*

Contribution from the Department of Chemistry, University of Houston, Houston, Texas 77004.
Received March 7, 1983

Abstract: The electrochemistry of $(TPP)Fe^{II}(NO)$ and $(OEP)Fe^{II}(NO)$ was investigated in nine nonaqueous solvents. In weakly binding solvents, such as dichloromethane or benzonitrile, five diffusion-controlled electron-transfer reactions were observed. Three of these reactions were oxidations. The remaining two reactions involved reversible electroreductions, either at the Fe(II) center or at the porphyrin ring. In strongly binding solvents, such as Me_2SO or pyridine, similar redox reactions were observed, but a number of chemical reactions were coupled to the electron-transfer steps. Formation of dinitrosyl complexes from either the unnitrosylated or mononitrosyl Fe(II) and Fe(III) complexes was characterized, and several stability constants measured. Finally, competitive ligation between different solvents and NO as axial ligand in each solvent system was studied along the series of oxidized, neutral, and reduced complexes.

During the last 15 years, a large number of studies have been published on the electrochemistry of (TPP)FeX and (OEP)FeX.[1] These studies have included investigations of the Fe(III)/Fe(II) reaction as well as oxidation to yield $[(TPP)FeX]^+$ or reduction to yield $[(TPP)Fe]^-$. In the former case, the reaction was initially postulated to be at the Fe(III) center, producing Fe(IV),[2,3] but this assignment now appears to be incorrect, and the actual oxidation probably occurs at the porphyrin ring.[4-6] For reduction,

(1) Kadish, K. M. *Phys. Bioinorg. Chem. Ser.* **1983**, 161-250.

(2) Felton, R. H.; Owen, G. S.; Dolphin, D.; Fajer, F. *J. Am. Chem. Soc.* **1971** *93*, 6332.

(3) Felton, R. H.; Owen, G. S.; Dolphin, D.; Forman, A.; Borg, D. C.; Fajer, J. *Ann. N.Y. Acad. Sci.* **1973**, *206*, 504.

0002-7863/83/1505-5610$01.50/0

the site of electron transfer is still a point of controversy and may be either at the Fe center or at the π ring system.[6-11]

A large number of electrochemical studies have concentrated on measuring potentials for oxidation or reduction of (TPP)FeX and (OEP)FeX as a function of either the associated counterion on Fe(III) or an axially bound nitrogenous base.[12-16] Very little, however, is known about the electrochemistry of these same iron porphyrins with diatomic molecules such as CS,[17-20] CO,[21] or, NO.[22-26]

Recently, the first reversible oxidation and reduction of (TPP)Fe(NO) and (OEP)Fe(NO) were reported in CH_2Cl_2 and pyridine.[24] Both of these complexes were stable in CH_2Cl_2, while in pyridine partial dissociation of NO occurred both before and after oxidation. In this publication, we wish to report a further characterization of (TPP)Fe(NO) and (OEP)Fe(NO) oxidation/reduction, as well as that for the dinitrosyl complexes (TPP)$Fe(NO)_2$ and (OEP)$Fe(NO)_2$.

Experimental Section

Chemicals. (TPP)Fe^{II}(NO) and (OEP)Fe^{II}(NO) were synthesized from (TPP)FeCl or (OEP)FeCl by literature methods.[23,25-27] Nitric oxide gas was purchased from Union Carbide Co. and passed through a dry ice–acetone bath (−78 °C) and KOH pellets prior to use. The solvents dichloromethane (CH_2Cl_2), dichloroethane (CH_2ClCH_2Cl), benzonitrile (PhCN), *n*-butyronitrile (*n*-PrCN), acetone (CH_3COCH_3), toluene ($PhCH_3$), and pyridine (py) were reagent grade quality, distilled from P_2O_5 or KOH,[28] and stored over 4-Å activated molecular sieves.

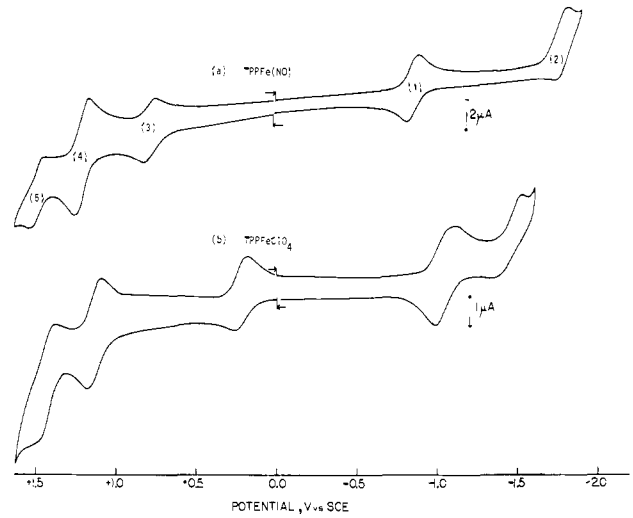

Figure 1. Cyclic voltammetry of (a) 1.09×10^{-3} M (TPP)Fe(NO) and (b) (TPP)$FeClO_4$ in PhCN–0.1 M TBAP. Scans were initiated in a positive or negative direction from 0.0 V and were carried out at 100 mV/s. Reactions 1–5 are given in the text.

Benzene, tetrahydrofuran (THF), dimethylacetamide (DMA), dimethylformamide (DMF), and dimethyl sulfoxide (Me_2SO) were spectrophotometric grade quality and stored over 4-Å molecular sieves. Unless mentioned otherwise, the solvents contained 0.1 M tetra-*n*-butylammonium perchlorate (TBAP) as supporting electrolyte, which was purchased from Eastman Kodak Co., twice recrystallized from ethyl alcohol, and dried in vacuo at 40 °C. In order to correct for liquid junction potential differences between solvents, all potentials were measured against the ferrocene/ferrocenium (Fc/Fc^+) couple. Ferrocene was purchased from Aldrich Chemical Co.

Instrumentation. Cyclic voltammetric measurements were made on Princeton Applied Research Models 174 or 173/175 polarographs/potentiostats or an IBM Model EC 225 electrochemical system. The first apparatus was used for sweep rates up to 0.5 V/s, and current–voltage curves were recorded on a PAR Model 9002A *X–Y* recorder. The two latter systems were used in connection with a Tektronix Model 5111 storage oscilloscope for sweep rates greater than 0.5 V/s. A three-electrode geometry was generally utilized. This consisted of two platinum button electrodes as the working and auxiliary electrodes and a commercial saturated calomel electrode (SCE) as the reference electrode. This latter electrode was separated from the bulk of the solution by a bridge filled with solvent and supporting electrolyte. Solutions in the bridge were changed periodically. Total volume utilized was 5–10 mL, and the porphyrin concentrations were maintained between 7×10^{-4} and 10^{-3} M.

For bulk controlled potential coulometry, a Princeton Applied Research Model 174 potentiostat/179 coulometer system was used. Current–time curves were recorded on a PAR Model 9002A *X–Y* recorder. Large coiled platinum wires served as both the anode and cathode, which were separated by means of a fritted glass or platinum wire bridge. A commercial saturated calomel electrode was again used as the reference electrode.

Thin-layer spectroelectrochemical measurements were performed with a PAR Model 173/175 potentiostat or an IBM EC 225 voltammetric analyzer coupled with a Tracor Northern 1710 holographic optical spectrometer/multichannel analyzer to obtain time-resolved spectral data. Spectra result from the signal averaging of a minimum of 100 sequential 5-ms spectral acquisitions. Each acquisition represented a single spectrum from 290 to 920 nm simultaneously recorded by a silicon diode array detector with a resolution of 1.2 nm per channel. The optically transparent thin-layer electrode (OTTLE) cell design has been described in former publications.[29,30] Sweep rates were below 5 mV/s, and a commercial saturated calomel electrode was used as the reference electrode.

A vacuum-tight cell was utilized for experiments conducted under a controlled atmosphere (inert gas or nitric oxide). This cell was also utilized for constant potential electrolysis. Its design was such that electronic absorption spectra could be acquired via an attached spectro-

(4) Gans, P.; Marchon, J.-C.; Reed, C. A.; Regnard, J.-R. *Nouv. J. Chim.* **1981**, *5*, 201.
(5) Goff, H. M.; Phillippi, M. A. *J. Am. Chem. Soc.* **1982**, *104*, 6026.
(6) Reed, C. A. In "Electrochemical and Spectrochemical Studies of Biological Redox Components", Kadish, K. M., Ed.; American Chemical Society: Washington, DC, 1982; Adv. Chem. Ser. No. 201, Chapter 15.
(7) Lexa, D.; Momenteau, M.; Mispelter, J. *Biochim. Biophys. Acta* **1974**, *338*, 151.
(8) Kadish, K. M.; Larson, G.; Lexa, D.; Momenteau, M. *J. Am. Chem. Soc.* **1975**, *97*, 282.
(9) Kadish, K. M.; Morrison, M. M.; Constant, L. A.; Dickens, L.; Davis, D. G. *J. Am. Chem. Soc.* **1976**, *98*, 8387.
(10) Fuhrhop, J. M.; Kadish, K. M.; Davis, D. G. *J. Am. Chem. Soc.* **1973**, *95*, 5140.
(11) Goff, H. M.; Phillippi, M. A.; Boersma, A. D.; Hansen, A. P. In ref 6, Chapter 16.
(12) Dolphin, D. Ed. "The Porphyrins"; Academic Press: New York, 1979; Vol. V.
(13) Phillippi, M. A.; Shimoura, E. T.; Goff, H. M. *Inorg. Chem.* **1981**, *20*, 1322.
(14) Bottomley, L. A.; Kadish, K. M. *Inorg. Chem.* **1981**, *20*, 1348.
(15) Kadish, K. M.; Bottomley, L. A.; Beroiz, D. *Inorg. Chem.* **1978**, *17*, 1124.
(16) Walker, F. A.; Barry, J. A.; Balke, V. L.; McDermott, G. A.; Wu, M. Z.; Linde, P. F. In ref 6, Chapter 17.
(17) Buchler, J. W.; Kokish, W.; Tonn, B.; *Z. Naturforsch., B: Anorg. Chem., Org. Chem.* **1978**, *33B*, 1371.
(18) Mansuy, D.; Battioni, J. P.; Chottard, J. C. *J. Am. Chem. Soc.* **1978**, *100*, 4311.
(19) Scheidt, W. R.; Geiger, D. K. *Inorg. Chem.* **1982**, *21*, 1208.
(20) Mansuy, D.; Lexa, D.; Saveant, J. M. *J. Chem. Soc., Chem. Commun.* **1981**, 888.
(21) Wayland, B. B.; Mehne, L. F.; Swartz, J. *J. Am. Chem. Soc.* **1978**, *100*, 2379.
(22) Wayland, B. B.; Minkiewicz, J. W.; Abd-Elmageed, M. E. *J. Am. Chem. Soc.* **1974**, *96*, 2795.
(23) Wayland, B. B.; Olson, L. W. *J. Chem. Soc., Chem. Commun.* **1973**, 897.
(24) Olson, L. W.; Schaeper, D.; Lançon, D.; Kadish, K. M. *J. Am. Chem. Soc.* **1982**, *104*, 2042.
(25) Frisse, M. E.; Scheidt, W. R. *J. Am. Chem. Soc.* **1975**, *97*, 17.
(26) Buchler, J. W.; Lay, K. L. *Z. Naturforsch., B: Anorg. Chem., Org. Chem.* **1975**, *30*, 385.
(27) Spaulding, L. D.; Chang, C. C.; Yu, N. T.; Felton, R. H. *J. Am. Chem. Soc.* **1975**, *97*, 2517.
(28) Perrin, D. D.; Armarego, W. L. F.; Perrin, D. R. "Purifications of Laboratory Chemicals", 2nd ed.; Pergamon Press: Oxford, 1980.
(29) Rhodes, R. K.; Kadish, K. M. *Anal. Chem.* **1981**, *53*, 1539.
(30) Rhodes, R. K.; Kadish, K. M. *Inorg. Chem.* **1981**, *20*, 2961.

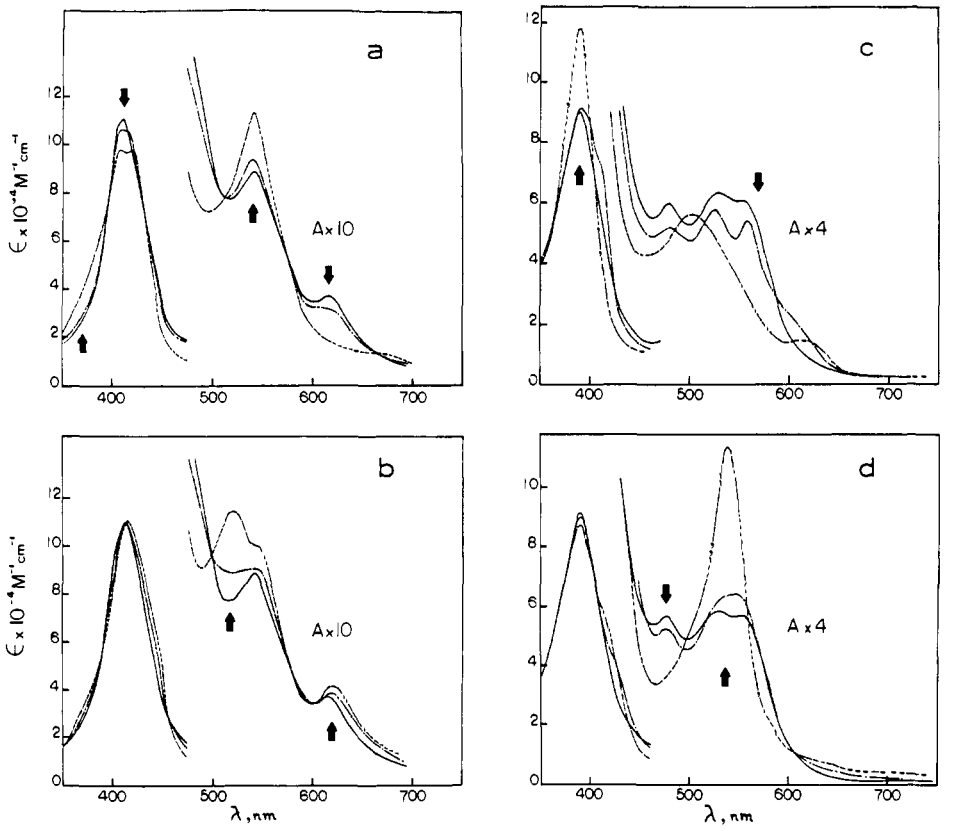

Figure 2. Time-resolved electronic absorption spectra taken at an OTTLE during the controlled potential oxidation of (a) (TPP)Fe(NO) and (c) (OEP)Fe(NO) and the controlled potential reduction of (b) (TPP)Fe(NO) and (d) (OEP)Fe(NO) in PhCN–0.3 M TBAP. The solid line represents the initial starting species.

photometric cell. The attached spectrophotometric cell had a 0.2-cm path length, and the overall minimum solution volume was 10 mL. Finally, unless specified otherwise, all potentials were reported vs. a saturated calomel electrode and are good to ±0.01 V.

Results and Discussion

Electrochemistry in Benzonitrile. Figure 1 illustrates a typical cyclic voltammogram of (TPP)Fe(NO) in benzonitrile–0.1 M TBAP. Five well-defined, single electron-transfer processes are observed between +1.7 and −1.9 V vs. SCE. Reactions 1 and

$$(TPP)Fe(NO) + e \rightleftarrows [(TPP)Fe(NO)]^{1-} \quad (1)$$

$$[(TPP)Fe(NO)]^{1-} + e \rightleftarrows [(TPP)Fe(NO)]^{2-} \quad (2)$$

$$(TPP)Fe(NO) \rightleftarrows [(TPP)Fe(NO)]^{1+} + e \quad (3)$$

$$[(TPP)Fe(NO)]^{1+} \rightleftarrows [(TPP)Fe(NO)]^{2+} + e \quad (4)$$

$$[(TPP)Fe(NO)]^{2+} \rightleftarrows [(TPP)Fe(NO)]^{3+} + e \quad (5)$$

3 have been described in the literature when the solvent was CH_2Cl_2.[24] In this solvent the reduction was reported at −0.93 V and the oxidation at +0.74 V. In benzonitrile reduction of (TPP)Fe(NO) has shifted slightly to −0.88 V, while the oxidation occurs at +0.75 V. In addition to these two reversible processes, three further reversible waves are seen in benzonitrile. These are a reduction at −1.89 V (reaction 2) and two oxidations at +1.17 and +1.46 V (reactions 4 and 5).

Under the same experimental conditions (TPP)$FeClO_4$ also exhibits five redox processes, as shown in Figure 1. Three of these are reductions and two are oxidations. For (TPP)$FeClO_4$ one observes an Fe(III) ⇄ Fe(II) process (at +0.20 V), while with (TPP)Fe(NO) the corresponding reaction is an oxidation (at +0.75 V), most likely producing Fe(III). It is interesting to note that the two oxidations of (TPP)$FeClO_4$ (+1.13 and +1.43 V) and the last two oxidations of (TPP)Fe(NO) occur at virtually identical potentials. In contrast, differences in potential are observed between the other three reactions of these two complexes.

The data in Figure 1 provide strong evidence for stabilization of the Fe(II) oxidation state with respect to Fe(III) in (TPP)Fe(NO). As seen in this figure, the oxidation of (TPP)Fe(NO) is shifted by 550 mV from that of (TPP)Fe to yield (TPP)$FeClO_4$ (the actual observed reaction in this case is the Fe(III) ⇄ Fe(II) reduction). When compared to other forms of (TPP)FeX (where X = F^-, Cl^-, Br^-, or N_3^-),[14] this potential stabilization appears to be even greater. For example, (TPP)FeF is reduced at −0.57 V in PhCN,[14] so that the potential difference is 1.32 V between (TPP)FeF and (TPP)Fe(NO).

A large shift in potential is also observed for reduction of $[(TPP)Fe(NO)]^-$ (reaction 2) when compared to reduction of the unnitrosylated $[(TPP)Fe]^-$ species. This is evident in Figure 1, where the cathodic shift of potential is 440 mV. This large cathodic shift implies a substantial stabilization of $[(TPP)Fe(NO)]^-$ relative to $[(TPP)Fe(NO)]^{2-}$ and also provides evidence that NO dissociation does not occur upon formation of $[(TPP)Fe(NO)]^-$.

Much smaller shifts in potential are observed for the first reduction of (TPP)Fe(NO) (reaction 1) when compared to (TPP)Fe. In PhCN the difference in potential amounts to only 180 mV, but is in a direction (anodically) consistent with stabilization of the $[(TPP)Fe(NO)]^-$ product. This stabilization of $[(TPP)Fe(NO)]^-$ is also evident by the 440-mV cathodic shift in reaction 2 and is not unexpected since addition of an electron to (TPP)Fe(NO) produces what should be a stable 18-d electron configuration.

Bulk controlled potential electrolysis and thin-layer spectroelectrochemical experiments were carried out to characterize the products of reactions 1 and 3. Bulk oxidation of (TPP)Fe(NO) did not quantitatively produce $[(TPP)Fe(NO)]^+$ but, rather, gave (TPP)$FeClO_4$ or $((TPP)Fe)_2O$, depending upon solution conditions. It has already been reported[24] that controlled potential reduction in a bulk cell showed no change in the visible spectra, even after the passage of up to 10 electrons, and it was suggested that $[(TPP)Fe(NO)]^-$ reconverted to (TPP)Fe(NO) by a catalytic process.

Table I. Characteristic UV-Vis Absorption Band of PorFe, PorFe(NO), and PorFe(NO)$_2$ in Various Solvents Containing 0.1 M Supporting Electrolyte and Their Respective Oxidation and/or Reduction Products

porphyrin ring	charge	compound[a]	solvent	Soret band ($\epsilon \times 10^{-4}$)	visible band ($\epsilon \times 10^{-3}$)
TPP^{2-}	+	$[(TPP)Fe]^+$	toluene[b]	405 (10)	515 (8), 565 (6), 610 (2)
		$[(TPP)Fe(NO)]^+$	PhCN	410 (9.9), 423 (9.7)	539 (11.4), 670 (0.8)
		$[(TPP)Fe(NO)_2]^+$	CH_2Cl_2	375 (10), 430 (11.2)	548 (13)
	0	(TPP)Fe	$EtCl_2$[c]	417 (8.0), 443 (6.5)	537 (9)
		(TPP)Fe(NO)	PhCN	410 (11)	540 (9), 610 (4)
		$(TPP)Fe(NO)_2$	CH_2Cl_2	433 (19)	545 (12.9), 581 (sh)
	−	$[(TPP)Fe]^-$	THF[d]	390, 423	510, 581 (sh), 608, 689
		$[(TPP)Fe(NO)]^-$	PhCN	414 (11)	517 (11), 539 (sh), 618 (3.6)
OEP^{2-}	+	$[(OEP)Fe]^+$	CH_2Cl_2[e]	380 (11.3)	500 (9.2), 633 (3.2)
		$[(OEP)Fe(NO)]^+$	PhCN	396 (10)	502 (8.5), 626 (2.4)
	0	(OEP)Fe(NO)	PhCN	394 (8.4)	481 (12.6), 530 (12), 552 (11.4)
		$(OEP)Fe(NO)_2$	PhCN	415 (12.7)	529 (13.7), 560 (14.7), 635 (0.9)
	−	$[(OEP)Fe(NO)]^-$	PhCN	394 (8.4)	541 (26), 581 (8.2)

[a] Associated TBA^+ or ClO_4^- counterions may be present with cationic or anionic species. [b] Values presented are for $TPPFeClO_4$, in the absence of supporting electrolyte. [c] Kadish, K. M.; Rhodes, R. K. *Inorg. Chem.* 1983, *22*, 1090. [d] Reference 6. [e] Dolphin, D. H.; Sams, J. R.; Tsin, T. B. *Inorg. Chem.* 1977, *16*, 711.

In contrast to these results, cyclic voltammetry experiments at an OTTLE show two reversible one-electron transfers generating $[(TPP)Fe(NO)]^+$ and $[(TPP)Fe(NO)]^-$. Although both reductions are spectrally reversible, the $[(TPP)Fe(NO)]^+$ complex formed by oxidation of (TPP)Fe(NO) is only rereduced to the starting material by 90–95% with the remaining 5–10% of $[(TPP)Fe(NO)]^+$ decomposing into $((TPP)Fe)_2O$. The electronic absorption spectra of $[(TPP)Fe(NO)]^+$ and $[(TPP)Fe(NO)]^-$ are presented in Figure 2, parts a and b, and the maximum wavelengths and molar absorptivities are listed in Table I. Also included in Figure 2, parts c and d, and Table I are the spectral properties of $[(OEP)Fe(NO)]^+$ and $[(OEP)Fe(NO)]^-$, which were electrochemically generated in a thin-layer cell and had similar stability to $[(TPP)Fe(NO)]^+$ and $[(TPP)Fe(NO)]^-$.

The spectrum of low-spin five-coordinate (TPP)Fe(NO) has been described in the literature.[23,25,31] In PhCN a Soret band is observed at 410 nm and two visible bands are located at 540 and 610 nm. Upon oxidation, the Soret band decreases slightly in intensity and appears to consist of two closely spaced bands. The longest wavelength band completely disappears, while the band at 540 nm increases in intensity. A small band also appears at 670 nm. Two isosbestic points are present at 505 and 565 nm, indicating the presence of only [(TPP)Fe(NO)] and $[(TPP)Fe(NO)]^+$ in solution.

The spectra obtained during controlled potential reduction of (TPP)Fe(NO) in an OTTLE are shown in Figure 2b. Very little change occurs in the Soret region, and a new band appears at 570 nm. Again, isosbestic points are obtained at 495, 565, and 605 nm, indicating only (TPP)Fe(NO) and $[(TPP)Fe(NO)]^-$ are present in solution. The slight change of Soret band position and intensity with addition of an electron suggests that the reduction does not occur at the π ring system but, rather, at the iron center or at the coordinated NO molecules. This suggestion is also consistent with the lack of broad absorption peaks in the visible region that would be characteristic of an anion radical.[32]

A similar invariance in position and intensity of the Soret peak is observed during formation of $[(OEP)Fe(NO)]^-$ from (OEP)Fe(NO) (Figure 2d). There is, however, a large increase in the intensity of the visible bands such that the final $[(OEP)Fe(NO)]^-$ product has a peak at 541 nm, which is twice the molar absorptivity of that observed at 530 and 552 nm for (OEP)Fe(NO). The same spectrum of $[(OEP)Fe(NO)]^-$ has been obtained from bulk coulometric experiments by Fajer et al.[33]

Finally, the oxidation of (OEP)Fe(NO) to yield $[(OEP)Fe(NO)]^+$ is shown in Figure 2c. The spectral changes obtained during controlled potential oxidation are more complex and suggest the possibility of intermediates. The final $[(OEP)Fe(NO)]^+$ product is identical with that obtained by Fajer[33] and does not have characteristics matching either $[(OEP)Fe]^+$ or (OEP)FeX complexes.

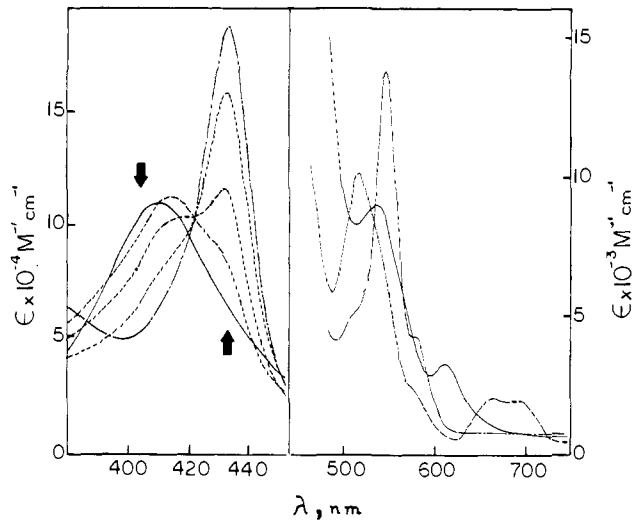

Figure 3. Spectral changes of (TPP)Fe(NO), during a titration with NO gas, in toluene. For the Soret region, $[(TPP)Fe(NO)] = 2.5 \times 10^{-5}$ M and total NO pressure introduced = 0, 29, 51, 81, and 760 mmHg. For the visible region, $[(TPP)Fe(NO)] = 3.5 \times 10^{-5}$ M and total NO pressure introduced = 0, 55, and 245 mmHg. The important species are represented as (—) (TPP)Fe(NO), (---) intermediate; (— — —) $(TPP)Fe(NO)_2$.

Dinitrosyliron(II) Complexes. The first qualitative characterization of $(TPP)Fe(NO)_2/(TPP)Fe(NO)$ equilibria was reported at 293 and 77 K in toluene by Wayland and Olson.[31] In this study a pressure of 400 mm NO resulted in conversion of (TPP)Fe(NO) to $(TPP)Fe(NO)_2$ as shown in eq 6. We have

$$(TPP)Fe(NO) + NO \rightleftarrows (TPP)Fe(NO)_2 \qquad (6)$$

repeated these experiments in toluene with an aim toward calculating the equilibrium constant for the above reaction and at the same time toward knowing the correct NO pressure for performing the electrochemistry of $(TPP)Fe(NO)_2$. These data are shown in Figure 3, which illustrates changes in the electronic absorption spectra at 25 °C during a titration of (TPP)FeNO with NO gas.

Suprisingly, no isosbestic point was observed between the initial $(TPP)Fe^{II}(NO)$ species spectrum and that for $(TPP)Fe(NO)_2$. However, a clear isosbestic point did appear between the final $(TPP)Fe(NO)_2$ spectrum and the spectrum of an intermediate species, generated upon introduction of a low pressure of NO gas (<120 mmHg). This new species is characterized by two main bands at 415 and 513 nm and two smaller bands at 662 and 690

(31) Wayland, B. B.; Olson, L. W. *J. Am. Chem. Soc.* **1974**, *96*, 6037.
(32) Fuhrhop, J-H. *Struct. Bonding (Berlin)* **1976**, *18*, 1.
(33) Fajer, J., private communication.

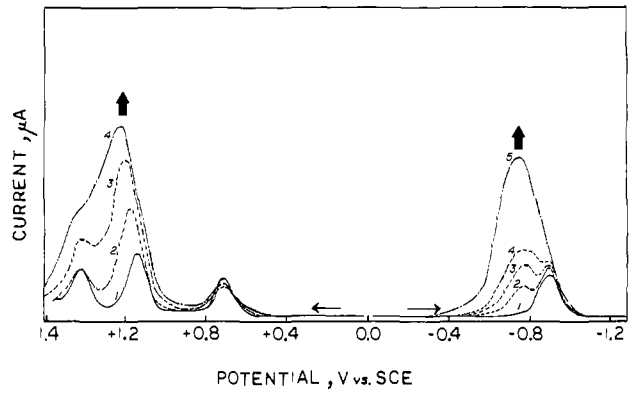

Figure 4. Differential pulse polarography (scan rate: 10 mV/s) of 10^{-3} M (TPP)Fe(NO), during a titration by NO gas, in PhCN–0.1 M TBAP. Total NO pressure introduced: (1) 0, (2) 83, (3) 149, (4) 252, and (5) 760 mmHg.

nm. The spectrum of this intermediate very closely resembles that of an Fe(III) high-spin species, especially in the region 600–700 nm.

All attempts to isolate or characterize this intermediate have failed to date, and the identity of this species remains unknown. There is no doubt that the original spectrum is that of (TPP)Fe(NO) and that the final product is that of (TPP)Fe(NO)$_2$. Furthermore, analysis of the spectral data at λ = 545 and 433 nm using Benesi–Hildebrandt type plots[34] gave straight line slopes, suggesting the addition of 1.8 ± 0.3 NO molecules when A_0 was taken as the spectral maxima of the intermediate (which is in equilibrium with (TPP)Fe(NO)$_2$). Similar spectral analysis using A_0 as that for (TPP)Fe(NO) absorbance resulted in plots of nonintegral slopes and, in any event, is theoretically invalid since this species is not in equilibrium with the product of NO addition. It should also be pointed out that the intermediate gave electrochemistry similar to that for (TPP)Fe(NO) and (TPP)Fe(NO)$_2$; this is discussed in the following sections.

Electrochemistry of (TPP)Fe(NO) and (TPP)Fe(NO)$_2$ under NO Atmosphere. Cyclic voltammetry and differential pulse polarography of (TPP)Fe(NO) and (OEP)Fe(NO) were carried out under NO pressures ranging from 0 to 760 mmHg. Under these conditions the electrochemistry of both the mono- and dinitrosyl ligand may be investigated. A typical set of differential pulse polarograms between +1.4 and −1.2 V is shown in Figure 4. In the absence of NO gas one reduction at −0.88 V and three oxidations (at +0.75, +1.17, and +1.46 V) are observed. Upon introduction of a positive NO pressure into the cell, two irreversible waves appear, at +1.20 and −0.80 V vs. SCE, corresponding to the respective oxidation and reduction of NO in solution. This was ascertained by the observed linear relationship between the cathodic and anodic wave peak height and the NO partial pressure. The large current for NO reduction makes the determination of $E_{1/2}$ by cyclic voltammetry for reduction of (TPP)Fe(NO)$_2$ very difficult at low NO pressures and almost impossible at NO pressures higher than 400 mmHg. However, over a limited range of NO pressures where (TPP)Fe(NO)$_2$ exists in solution (as verified by spectral data), the half-wave potentials for the first reduction and oxidation of this complex may be determined by differential pulse polarography.

As shown in Figure 4, the potentials do not appear to shift as a function of NO pressure. In fact under 1 atm (760 mmHg) of NO gas, the half-wave potential for the oxidation of (TPP)Fe(NO)$_2$ appears to remain within 20 mV of the potential for (TPP)Fe(NO) oxidation under an N_2 atmosphere. This indicates either an equal stability of the mono- and dinitrosyl species or a rapid coversion of (TPP)Fe(NO)$_2$ to (TPP)Fe(NO) before electron transfer. On the basis of the data obtained for (OEP)Fe(NO) and (OEP)Fe(NO)$_2$ oxidation under an NO atmosphere (see following section) this latter suggestion seems to be the more likely possibility. Furthermore, on the cathodic sweep, the first reduction also appears to remain reversible with an invarient half-wave potential of −0.88 V, even at high pressures of NO gas. Again, one is unable to differentiate between rapid conversion of (TPP)Fe(NO)$_2$ to (TPP)Fe(NO) before electron transfer and a condition where both species have identical reduction potentials.

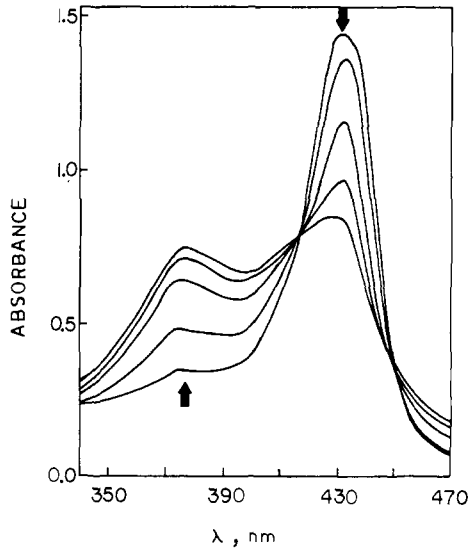

Figure 5. Time-resolved electronic absorption spectrum during the bulk controlled potential oxidation of (TPP)Fe(NO)$_2$ under 760 mmHg of NO gas in CH_2Cl_2, 0.1 M TBAP. Total electrolysis time 47 min.

Table II, Half-Wave Potentials (V vs. SCE) for the First Oxidation and First Reduction of (OEP)Fe(NO), in Five Nonaqueous Solvents

solvent	first oxidation	first reduction
CH_2Cl_2	+0.60[a]	−1.10[a]
PhCN	+0.69	−1.08
n-PrCN	+0.62	−1.07
DMF	(+0.56)[b]	−1.00
py	(+0.57)[a,b]	−1.10[a]

[a] Reference 24. [b] Potentials are quoted for $E_{p,a}$ at 200 mV/s; no reversible wave was observed in these solvents.

Bulk coulometry was carried out in PhCN to spectrally characterize the electrochemically generated [(TPP)Fe(NO)$_2$]$^+$, under 760 mm of NO gas. Both oxidation and rereduction were reversible one-electron processes and gave the electronic absorption spectrum shown between 340 and 470 nm (Figure 5). As seen in this figure, there is clear conversion of (TPP)Fe(NO)$_2$ to [(TPP)Fe(NO)$_2$]$^+$. The spectrum of the oxidized dinitrosyl product agrees with the spectrum of the same species produced by addition of NO gas to (TPP)FeClO$_4$ in CH_2Cl_2.[24] Well-defined isosbestic points in Figure 5 characterize the absence of any coupled chemical reactions or intermediate species formation. Both (TPP)Fe(NO)$_2$[31,35] and [(TPP)Fe(NO)$_2$]$^+$ClO$_4^-$[24] exhibit two N–O stretching frequencies in the infrared spectrum. [(TPP)Fe(NO)$_2$]$^+$ClO$_4^-$ appears to possess very similar linear (Fe–N–O) bonds for both axial ligands,[24] since both its stretching frequencies are close to 1900 cm^{-1}, while (TPP)Fe^{II}(NO)$_2$ is known to have a bent and a linear (Fe–N–O) bond.[31]

Electrochemistry of (OEP)Fe(NO) and (OEP)Fe(NO)$_2$ under NO Atmosphere. The electrochemistry of (OEP)Fe(NO) was initially described in CH_2Cl_2.[24] Similar to (TPP)Fe(NO) five oxidation–reduction reactions were observed whose potentials are listed in Table II. As expected, all of the potentials were shifted cathodically from those of (TPP)Fe(NO) due to the greater electron density of the OEP^{2-} ring. Both the oxidation and reduction are reversible, and the spectra of the products in PhCN

(34) Benesi, H. A.; Hildebrand, J. H. *J. Am. Chem. Soc.* **1949**, *71*, 2073.

(35) Wayland, B. B.; Newman, A. R. In "Porphyrin Chemistry Advances"; Longo, F. R., Ed.; Ann Arbor Sciences: 1979; p 245.

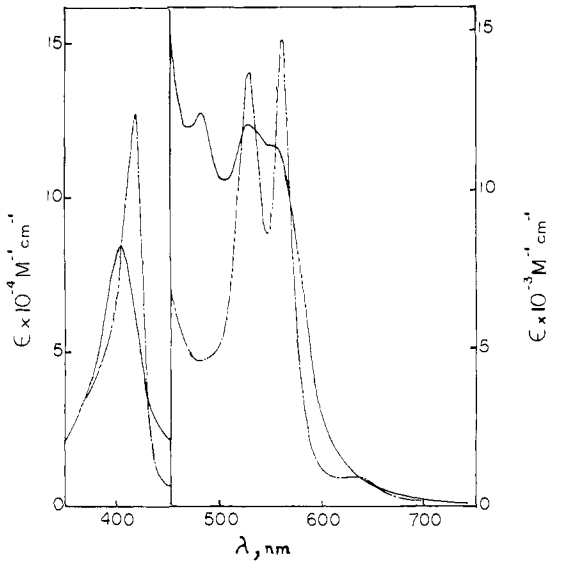

Figure 6. Electronic absorption spectra of (OEP)Fe(NO) (—) and (OEP)Fe(NO)$_2$ (– – –), in PhCN. For the Soret region, [(OEP)Fe(NO)] = 1.4 × 10^{-5} M and P_{NO} = 120 mmHg. For the visible region, [(OEP)Fe(NO)] = 1.4 × 10^{-4} M and P_{NO} = 305 mmHg.

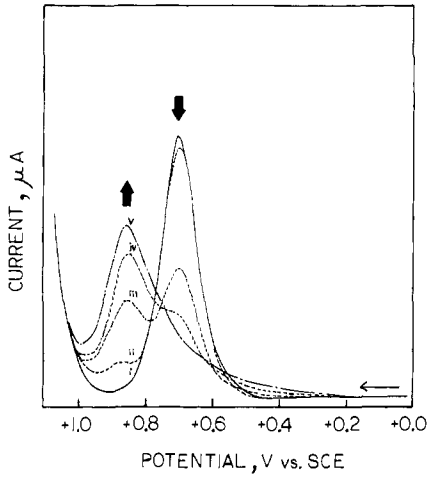

Figure 7. Differential pulse polarography (scan rate: 10 mV/s) of 10^{-3} M (OEP)Fe(NO), during a titration by NO gas, in PhCN–0.1 M TBAP. Total NO pressure introduced: (1) 0, (2) 36, (3) 69, (4) 225, and (5) 760 mmHg.

under an N_2 atmosphere are shown in Figure 2. Similar electrochemical and spectral experiments of (OEP)Fe(NO) were carried out under a controlled NO atmosphere in PhCN. Addition of NO to (OEP)Fe(NO) may be described by reaction 7.

$$\text{(OEP)Fe(NO)} + \text{NO} \rightleftarrows \text{(OEP)Fe(NO)}_2 \qquad (7)$$

Spectra for the initial (OEP)Fe(NO) and the final (OEP)-Fe(NO)$_2$ are shown in Figure 6, and the spectral wavelengths and molar absorptivities are listed in Table I. At an initial 10^{-4} M (OEP)Fe(NO) concentration, complete conversion to the dinitrosyl occurred with 150–250 mm NO gas, while at a 10^{-3} M concentration of (OEP)Fe(NO) approximately 760 mm NO was needed for conversion to the dinitrosyl complex.

The electrochemistry of (OEP)Fe(NO) and (OEP)Fe(NO)$_2$ was investigated in PhCN over a range of NO pressures between 0 and 760 mm, and the results are shown in Figures 7 and 8 for the oxidation process only. Figure 7 illustrates the differential pulse polarograms of (OEP)Fe(NO) or (OEP)Fe(NO)$_2$ at several NO pressures while Figure 8 shows a cyclic voltammogram of the same species at a NO pressure of 760 mmHg. Similar to the results shown in Figure 3, a large peak was observed at +1.20 V for the oxidation of NO. However unlike the results for (TPP)Fe(NO) and (TPP)Fe(NO)$_2$, oxidations of OEPFe(NO)

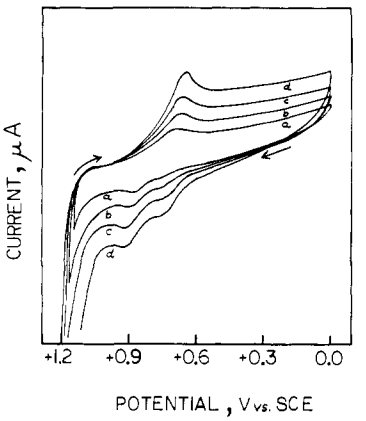

Figure 8. Cyclic voltammetry of 10^{-3} M (OEP)Fe(NO) under 760 mn of NO gas in PhCN–0.2 M TBAP. Scan rates: (a) 0.20, (b) 0.50, (c) 1.00, and (d) 2.00 V/s.

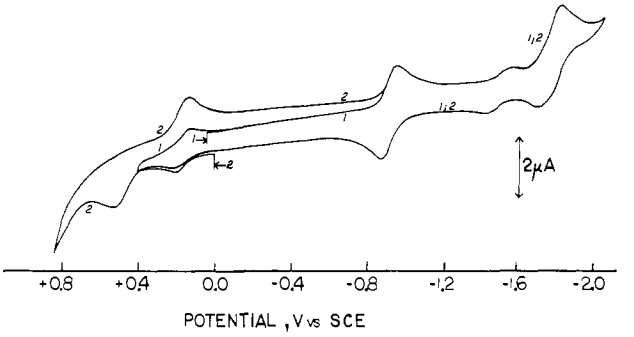

Figure 9. Cyclic voltammetry of 1.14 × 10^{-3} M (TPP)Fe(NO) in py–0.1 M TBAP. Scan rate: 100 mV/s.

and (OEP)Fe(NO)$_2$ appear to occur at different potentials. The former complex is reversibly oxidized at $E_{1/2}$ = +0.69 N, while the latter is oxidized at E_p = +0.90 V. This conversion of (OEP)Fe(NO) to (OEP)Fe(NO)$_2$ is observed on the differential pulse polarograms (Figure 7) illustrated as a function of changing NO pressures. The currents for the two processes are not equal due to the irreversibility of the second process, which gives theoretically predicted[36] smaller currents than for a reversible process of the same species.

Only a single rereduction is observed for oxidation of (OEP)Fe(NO)$_2$ by cyclic voltammetry. This reduction is found at an E_p = 0.66 V (Figure 8), at 0.10 mV/s, and suggests that dissociation of an NO group from [(OEP)Fe(NO)$_2$]$^+$ occurs before reduction.

Thus, on the basis of the results of Figures 7 and 8, the overall oxidation/reduction scheme may be written as

$$\begin{array}{ccc} \text{(OEP)Fe(NO)} & \rightleftharpoons & \text{(OEP)Fe(NO)}_2 \\ E_{1/2} = 0.69\ \text{V} \downarrow\uparrow -e & & -e \uparrow\downarrow E_p = 0.90\ \text{V} \\ [\text{(OEP)Fe(NO)}]^+ & & [\text{(OEP)Fe(NO)}_2]^+ \end{array}$$

In this scheme both (OEP)Fe(NO) and (OEP)Fe(NO)$_2$ are oxidized to the respective [(OEP)Fe(NO)]$^+$ and [(OEP)Fe(NO)$_2$]$^+$ complexes. This latter dinitrosyl iron(III) complex is not stable and converts rapidly to [(OEP)Fe(NO)]$^+$, which is then reduced to (OEP)Fe(NO) at $E_{1/2}$ = 0.69 V. This neutral species can then reconvert to (OEP)Fe(NO)$_2$, which is in the bulk of solution. The fact that two oxidation waves are observed in this case but not for the case of (TPP)Fe(NO) and (TPP)Fe(NO)$_2$ may be due either to an equilibrium greatly displaced toward the dinitrosyl complex or to slow dissociation kinetics of (OEP)Fe(NO)$_2$.

Electrochemistry of (TPP)Fe(NO) in Neat Pyridine. A cyclic voltammogram of (TPP)Fe(NO) in pyridine containing 0.1 M

(36) Nicholson, R. S.; Shain, I. *Anal. Chem.* **1964**, *36*, 706.

Table III. Half-Wave Potentials (V vs. SCE) for the Five Electron Transfers of (TPP)Fe(NO), in Eight Nonaqueous Solvents

solvent	dielectric constant	DN[e]	reactions[a] 5	4	3	1	2	$E_{1/2}(Fc^+/Fc)$
CH_2ClCH_2Cl	10.4	0.0	+1.35	+1.12	+0.69	−0.90		+0.47
CH_2Cl_2	8.9	0.0	+1.39	+1.18	+0.74	−0.93	−1.78[c]	+0.49
PhCN	25.2	11.9	+1.46	+1.17	+0.75	−0.88	−1.89	+0.43
THF	7.6	20.0		+1.01	+0.66	−0.95	−1.80	+0.52
DMF	36.7	26.6		+1.18	(+0.61)[d]	−0.76	−1.73	+0.51
DMA	37.8	27.8		+1.26	(+0.65)[d]	−0.75	−1.73	+0.54
Me_2SO	46.5	29.8		+0.98[b,c]	(+0.43)[b,d]	−0.75[b,c]	−1.66[b,c]	+0.47
py	12.4	33.1		+0.91	(+0.52)[d]	−0.91	−1.76	+0.53

[a] Reaction numbers are given in the text. [b] Poor solubility of (TPP)Fe(NO) in this solvent. [c] Data from differential pulse polarography at a Pt electrode; potential reported is E_p, at 5 mV/s. [d] Potentials are quoted for $E_{p,a}$ at 100 mV/s; no cathodic wave was observed in these solvents. [e] Gutmann, V. "The Donor-Acceptor Approach to Molecular Interactions"; Plenum: New York, 1978.

TBAP is presented in Figure 9. In this solvent the reacting nitrosyl species is (TPP)Fe(NO)(py), which is formed by addition of a sixth pyridine ligand to (TPP)Fe(NO).[37]

$$(TPP)Fe(NO) + py \rightleftarrows (TPP)Fe(NO)(py) \quad (8)$$

Two reversible reductions ($E_{1/2}$ = −0.91 and −1.76 V) and one irreversible oxidation (E_{pa} = +0.52 V at a scan rate of 0.10 V/s) of (TPP)Fe(NO)(py) are observed in Figure 9. In addition, an oxidation ($E_{1/2}$ = +0.17 V) and a reduction ($E_{1/2}$ = −1.50 V) of $(TPP)Fe(py)_2$ is also observed in Figure 9. These redox processes have been characterized in py, 0.1 M TBAP.[14] The $(TPP)Fe(py)_2$ in this present study is formed by the addition of a second py molecule to (TPP)Fe(py)(NO) that displaces NO from the complex.

$$(TPP)Fe(py)(NO) + py \rightleftarrows (TPP)Fe(py)_2 + NO \quad (9)$$

Confirmation of NO displacement at high py concentrations was obtained during spectral titrations of (TPP)Fe(NO) with pyridine in CH_2Cl_2. This is shown in Figure 10. Addition of one py molecule to (TPP)Fe(NO) (reaction 8) results in no significant spectral changes.[37] Addition of the second by molecule (reaction 9), however, produces the spectral changes shown in Figure 10. As seen in this figure, the bands characteristic of (TPP)Fe(NO) or (TPP)Fe(NO)(py) begin to change at 0.1 M pyridine in CH_2Cl_2 and only at 6 M pyridine are the spectral changes complete. Clear isosbestic points are obtained at all concentrations of pyridine. Analysis of the spectra using Benesi–Hildebrandt methods[34] gave a characteristic slope of 1.0 and a log K_2 = −0.2 for reaction 9 in CH_2Cl_2. This stability constant is smaller in neat pyridine than in CH_2Cl_2, as evidenced by the fact that (TPP)Fe(NO)(py) still exists in large quantities.

From the ratios of the experimentally measured cathodic peak currents at −0.91 V or the anodic peak currents at +0.17 and +0.52 V, an approximate value of log K_2 = −1.5 can be calculated for reaction 9. This calculation, which is only approximate, assumes that the diffusion coefficients of all species are identical in pyridine and that there is no conversion between bound NO and pyridine during the time scale of the experiment.

As seen in Figure 9 oxidation of (TPP)Fe(NO)(py) does not produce a stable nitrosyl product, but rather generates $[(TPP)Fe(py)_2]^+$, which is present in much smaller amounts when the anodic sweep is terminated at +0.40 V. Analysis of the shape and scan rate dependence for the peak at E_p = 0.52 V suggests an EC type mechanism[36] as shown below.

$$(TPP)Fe(py)(NO) \overset{-e}{\rightleftharpoons} [(TPP)Fe(py)(NO)]^+ \overset{py}{\underset{NO}{\rightleftharpoons}} [(TPP)Fe(py)_2]^+ \quad (10)$$

The displacement of NO by py on Fe(III) is consistent with the known binding properties of NO[31] and pyridine[38] for iron(III) porphyrins. Attempts were made to obtain reversible oxidations, but even at fast scan rates and low temperatures (−30 °C) no reverse peak was obtained.

(37) Tonn, B. thesis, Institut für Anorganische Chemie, Aachen, 1979.
(38) Bottomley, L. A.; Kadish, K. M. *Inorg. Chem.* **1980**, *19*, 832.

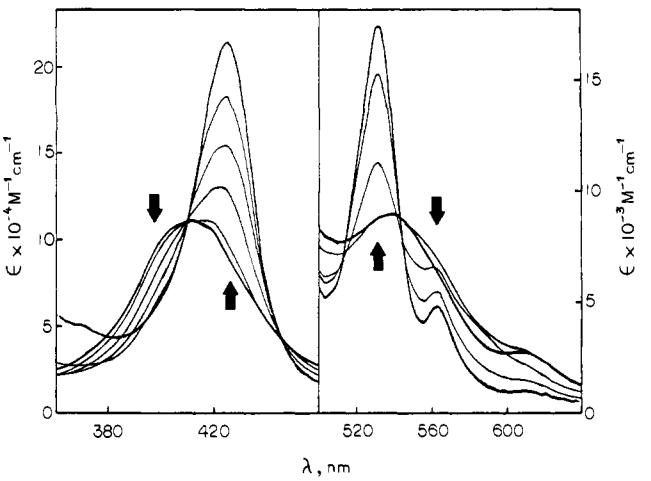

Figure 10. Spectral changes of 1.01 × 10^{-5} M (Soret band) and 1.22 × 10^{-4} M (visible bands) (TPP)Fe(NO) observed during titration by py in CH_2Cl_2–0.1 M TBAP. Total concentration of py in solution: 0, 0.10, 0.40, 1.41, 3.64, and 5.9 M for the Soret Band; 0, 0.12, 1.2, 1.7, and 2.3 M for the visible band.

Solvent Effects on Electrode Reactions. In order to better understand the effect of solvent binding, the electrode reactions of (TPP)Fe(NO) and (OEP)Fe(NO) were carried out in a variety of nonaqueous solvents. These solvents can be classified into three groups by comparison of their acid–base properties and their relative values of dielectric constants: the aprotic inert class I (CH_2ClCH_2Cl, CH_2Cl_2), the nondissociating basic protic class II (THF, py), and the dissociating aprotic class III (PhCN, DMF, DMA, Me_2SO).

In solvents of DN lower than 20 (CH_2ClCH_2Cl, CH_2Cl_2, and PhCN) all electrode reactions were reversible and there was no electrochemical evidence for unnitrosylated Fe(III) or Fe(II) complexes. These potentials are listed in Table III for (TPP)Fe(NO) and Table II for (OEP)Fe(NO). In solvents having a DN > 20, an equilibrium exists in solution between (TPP)Fe(NO) and (TPP)Fe(NO)(S), although the data indicate an almost equivalent spectrum for (TPP)Fe(NO) and (TPP)Fe(NO)(S). If (TPP)Fe(NO) is added to group II solvents such as THF or py an equilibrium exists between (TPP)Fe(NO)(S) and $(TPP)Fe(S)_2$. This is evidenced by new peaks appearing for $(TPP)Fe(S)_2$ reduction[14] and, in the case of pyridine, by an electronic absorption spectrum that indicates a mixture of (TPP)Fe(NO)(py) and $(TPP)Fe(py)_2$. This spectrum is shown in Figure 11d. The electronic absorption spectra in CH_2Cl_2, PhCN, and Me_2SO are shown in Figure 11a–c and are virtually identical, but different than that in pyridine.

The electrochemistry of (TPP)Fe(NO) is greatly dependent upon the solvent binding ability, as we have noted from the above discussion. The two reductions of (TPP)Fe(NO) [or (TPP)Fe(NO)(S)] and the second oxidation of the same complex(es) become easier as the dissociating ability of the solvent is increased. This effect is largest for the first reduction which has a maximum shift of 100 mV between solvents. In contrast, half-wave potentials

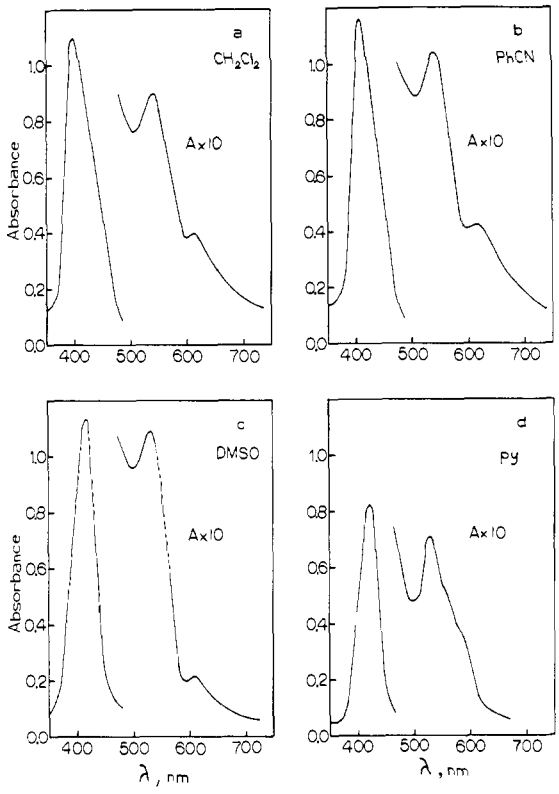

Figure 11. Electronic absorption spectra of (TPP)Fe(NO) in various solvents containing 0.1 M TBAP: (a) CH_2Cl_2, (b) PhCN, (c) Me_2SO, (d) py.

remain almost invariant in the nondissociating solvents of classes I and II. Also, it is of interest to note from Tables II and III that a larger solvent effect is noted for (TPP)Fe(NO)(S) than for (OEP)Fe(NO)(S).

Potentials for the first reduction of (TPP)Fe(NO) and (OEP)Fe(NO) can be compared to the potentials for (TPP)Fe and (OEP)Fe reduction in a number of solvents. An earlier study of solvent effects on the redox reactions of (TPP)Fe(S) and (TPP)Fe(S)$_2$ showed that $E_{1/2}$ (when corrected for liquid junction potential) was virtually independent of solvent.[14] This is not the case for (TPP)Fe(NO)(S) and (OEP)Fe(NO)(S). Binding of a solvent molecule results in an anodic shift of potential from that of (TPP)Fe(NO) or (OEP)Fe(NO) with the magnitude of the shift being dependent upon the solvent DN. The maximum potential difference of this shift is 150 mV between (TPP)Fe(NO) and (TPP)Fe(NO)(S) (where S = DMA or Me_2SO). A similar anodic shift is also observed for (OEP)Fe(NO)(S), but in this case the anodic shift was smaller in magnitude.

In conclusion, we have shown that the binding of one or two nitrosyl ligands to (TPP)Fe and (OEP)Fe generate dramatic shifts of redox potentials for oxidation and reduction of the stable Fe(II) complexes. For the case of (TPP)Fe(NO), the magnitude of shift in the Fe(III)/Fe(II) reaction with respect to (TPP)FeCl is approximately 1.0 V, independent of solvent. Similar values of $\Delta E_{1/2}$ are also observed between (OEP)Fe(NO) and (OEP)FeCl, but an even greater potential shift is observed after formation of (OEP)Fe(NO)$_2$, which is oxidized at a potential 200 mV anodic of (OEP)Fe(NO). These shifts of potential are comparable to those induced by the binding of CO to Fe(II),[1,39] but with NO as an axial ligand, stable oxidized complexes may be obtained. This is not true with CO, which does not bind to Fe(III). In this paper we have also spectrally identified the first reduced complex of Fe(II) with a bound axial ligand, $[PorFe(NO)]^{-1}$. Similar spectral identifications have been obtained for $[PorFe(NO)]^+$ and $[PorFe(NO)_2]^+$. These spectral and electrochemical characterizations of model Fe(II) complexes that have been oxidized or reduced are of importance in understanding the redox reactions of heme proteins with small diatomic molecules such as NO, CO, or O_2.

Acknowledgment. We are grateful for the financial support of this work from the National Institutes of Health (Grant GM 25172). We also with to thank Dr. S. Kelly for helpful discussions and R. Wilkins for making speciality electrochemical cells.

Registry No. (TPP)Fe(NO), 52674-29-0; (OEP)Fe(NO), 55917-58-3; (TPP)Fe(NO)$_2$, 53637-75-5; (OEP)Fe(NO)$_2$, 68879-28-7.

(39) Buchler, W. J.; Kokisch, W.; Smith, P. D. *Struct. Bonding (Berlin)* **1978**, *34*, 79.

Reduction Potentials for 2,2′-Bipyridine and 1,10-Phenanthroline Couples in Aqueous Solutions

C. V. Krishnan, Carol Creutz,* Harold A. Schwarz, and Norman Sutin

Contribution from the Department of Chemistry, Brookhaven National Laboratory, Upton, New York 11973. *Received February 7, 1983*

Abstract: From pulse-radiolysis studies of 2,2′-bipyridine (bpy), 1,10-phenanthroline (phen), and 4,4′-dimethyl-2,2′-bipyridine ($(CH_3)_2$bpy) and an analysis of the pH and free-energy dependence of the rate constants for quenching of poly(pyridine)-ruthenium(II) excited states by the above aromatic amines (L) and their protonated counterparts (LH^+, LH_2^{2+}), the following parameters concerning L and its one-electron reduction product $L^{-}\cdot$ have been deduced at 25 °C: for L = bpy, $pK_a(LH_2^{2+}) = 0.05$, $pK_a(LH^+) = 4.4$, $pK_a(LH_2^{+}\cdot) = 8.0$, $pK_a(LH\cdot) \simeq 24$, $E°(LH_2^{2+}-LH_2^{+}\cdot) = -0.50$ V, $E°(LH^+-LH\cdot) = -0.97$ V; for L = phen, $pK_a(LH_2^{2+}) = -0.2$, $pK_a(LH^+) = 4.9$, $pK_a(LH\cdot) \simeq 24$, $E°(LH_2^{2+}-LH_2^{+}\cdot) = -0.47$ V, $E°(LH^+-LH\cdot) = -0.85$ V; and for L = $(CH_3)_2$bpy, $pK_a(LH_2^{2+}) = 0.68$, $pK_a(LH_2^{+}\cdot) = 9.3$, $pK_a(LH\cdot) \simeq 25$, $E°(LH_2^{2+}-LH_2^{+}\cdot) = -0.54$ V, $E°(LH^+-LH\cdot) = -1.05$ V. The reduction potentials and other electron-transfer parameters of these and related couples are discussed.

The one-electron reduction of 2,2′-bipyridine (bpy) to $bpy^{-}\cdot$ is electrochemically reversible ($E_{1/2} = -2.13$ V vs. aqueous SCE) in acetonitrile[1] and *N*,*N*-dimethylformamide,[2] and the two-electron reduction process has been characterized in aqueous media.[3-5] Polarographic data have been reported for the one-electron process in water,[6] but the interpretation of these data is complicated by

(1) Tokel-Takvoryan, N. E.; Hemingway, R. E.; Bard, A. J. *J. Am. Chem. Soc.* **1973**, *95*, 6582.
(2) Saji, T.; Aoyagui, S. *J. Electroanal. Chem.* **1975**, *63*, 31.
(3) Erhard, H.; Jaenicke, W. *J. Electroanal. Chem.* **1975**, *65*, 675.
(4) Erhard, H.; Jaenicke, W. *J. Electroanal. Chem.* **1977**, *81*, 79.
(5) Erhard, H.; Jaenicke, W. *J. Electroanal. Chem.* **1977**, *81*, 89.
(6) Gurtler, O.; Dietz, K. P.; Thomas, P. *Z. Anorg. Allg. Chem.* **1973**, *398*, 217.

0002-7863/83/1505-5617$01.50/0